QUASI-STEADY-STATE PHOTOCONDUCTANCE, A NEW METHOD FOR SOLAR CELL MATERIAL AND DEVICE CHARACTERIZATION

Ronald A. Sinton

Sinton Consulting, San Jose, California, USA

Andres Cuevas and Michael Stuckings

Australian National University, Canberra, Australia

Abstract: This paper describes a new method for minority-carrier lifetime determination using a contactless instrument in a quasi-steady-state photoconductance mode. Compared to the more common transient photoconductance decay approach, the new technique permits the use of simpler electronics and light sources, yet has the capability to measure lifetimes in the nanosecond to millisecond range. In addition, by analyzing the quasi-steady-state photoconductance as a function of incident light intensity, an implicit I_{sc}-V_{oc} curve can be obtained for non-contacted silicon wafers and solar cell precursors.

Introduction: Measurements of minority-carrier lifetime in silicon wafers are extremely valuable for process control and device optimization as well as for material and device physics research. Photoconductance decay is a commonly used method based on analyzing photoconductance decay transients after a very short light pulse from a laser, flash lamp, LED array or laser diode. The effective lifetime is obtained from the slope of the decay curve:

$$t_{effective} = \Delta n/(d(\Delta n)/dt \qquad 1)$$

This method has been exhaustively developed. Many techniques have been used to sense the photoconductivity without contacting the wafer including microwave reflectance, capacitive coupling, and the use of a coil to couple inductively the wafer conductivity. For a typical induction-coupling apparatus with a 5 μs light pulse and a RF frequency of 10 MHz, effective lifetimes greater than 50 μs are easily and accurately measured [1]. For lifetimes down to the 10 ns range, shorter light pulses and higher frequency RF circuits can be used [2] For effective lifetimes shorter than 50 μs on silicon wafers, surface recombination transients and minority-carrier spreading effects are present that complicate the interpretation and application of the measurement results.

Steady-State Photoconductance Method

An alternative to the transient method is to measure the photoconductance under steady-state illumination. The photogenerated excess carrier density, $\Delta n = \Delta p$, results in an increase in wafer conductance given by:

$$\sigma_L = q(\Delta n \mu_n + \Delta p \mu_p)W = q\Delta n(\mu_n + \mu_p)W . \qquad 2)$$

Where W is the wafer width. The mobilities are a function of both the doping and the injection level and can be found in the literature. The equation can be iterated to find both Δn and $(\mu_n + \mu_p)$ consistent with the measured conductance.

In the steady state, the generation of electron-hole pairs must be in balance with the recombination of these same pairs. Expressing the photogeneration and recombination rates as current densities.

$$J_{photogeneration} = J_{recombination} \qquad 3)$$

The total recombination in the wafer can be expressed in terms of an effective minority carrier lifetime, τ_{eff} :

$$J_{ph} = \Delta n q W/\tau_{eff} \qquad 4)$$

This equation assumes that Δn is approximately uniform across the wafer. Substituting sheet conductance for Δn,

$$\tau_{eff} = \sigma_L / (J_{ph}(\mu_n + \mu_p)) \qquad 5)$$

The conductance and the incident light intensity can be measured using a calibrated instrument and a reference solar cell next to the sample of interest, respectively. At one sun illumination, the photogeneration, J_{ph}, for a 380 μm thick silicon wafer is approximately 38 mA/cm^2. This value for J_{ph} can be adjusted for different front surface reflection, wafer thickness, light-trapping features or illumination spectrum and can be easily estimated using available computer programs or lookup tables. Even after these possible variations have been considered, J_{ph} generally lies within a tight range of 34-42 mA/cm^2. Note that Eq. 5 does not depend on the details of the minority-carrier distribution, except for the very-weak dependence introduced by evaluating $(\mu_n + \mu_p)$ at the average Δn.

0-7803-3166-4/96/$5.00 © 1996 IEEE

25th PVSC; May 13-17, 1996; Washington, D.C.

Quasi-Steady-State Photoconductance Technique

A convenient implementation of the steady-state approach described above is to use a light pulse that varies *very slowly* compared to the effective lifetime of the wafer. This offers an expedient method for obtaining the photoconductance under a large range of illumination intensities in a short time without significant sample heating. Analysis of the photoconductance as a function of irradiance provides additional useful information, including an implicit I-V characteristic curve, as shown below, and the ability to separate out different recombination mechanisms [3].

In this technique, the effective lifetime is determined at every light intensity following the procedure and equations outlined in the previous section. Examples of photoconductance and effective lifetime data from this technique are shown in Figs. 1 and 2.

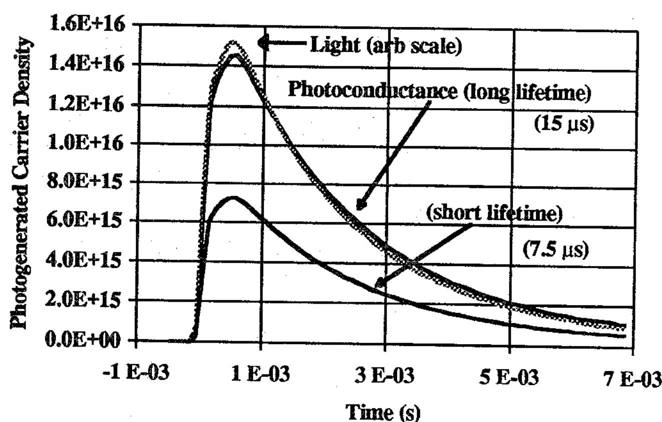

Fig. 1. Raw data from quasi-steady-state photoconductance measurements. The lifetime is proportional to the photoconductance amplitude.

Compared to a transient decay approach, the quasi-steady-state method allows the measurement of very low lifetimes without fast electronics or short light pulses. The range of measurable lifetimes is only limited by signal strength. The sensitivity of the instrument used here was 27 V/S. Considering that 5 mV constitutes an adequate signal, eq. 5 implies that the detection limit of this instrument is 3 μs at one sun illumination, or 3 ns at 1000 suns.

An example of the capability to measure low lifetimes is given in Fig. 2. This small-grained polysilicon wafer with boron diffusions on both surfaces has a 345-ns lifetime.

The quasi-steady-state photoconductance data implicitly contains information about the I_{SC}-V_{OC} current voltage characteristics of the device or structure being measured.

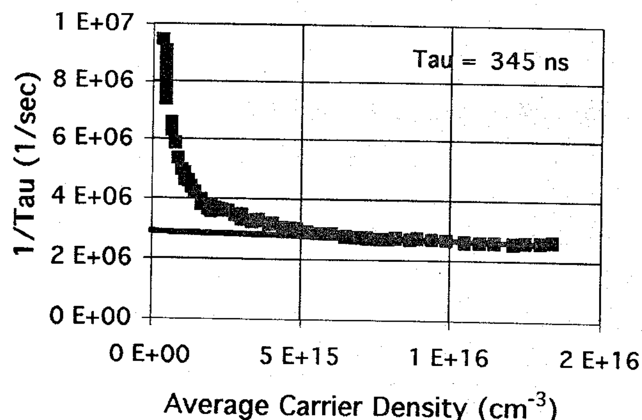

Fig. 2. The inverse of effective lifetime vs. minority-carrier density for a 345 ns small-grained multicrystalline silicon sample.

The short-circuit current is implied by the irradiance. The excess carrier density implies an open circuit voltage, the separation of the quasi-Fermi levels. Photoconductance and voltage are both measures of the same excess minority-carrier density. For a solar cell made on a p-type wafer, the implicit voltage is:

$$V_{OC} = (kT/q)\ln((\Delta n)(N_A+\Delta p)/n_i^2) \qquad 6)$$

If the surfaces are passivated and the diffusion length is greater than the wafer thickness this simple conversion to implied voltage based on assuming that Δn is uniform across the wafer is accurate. In other cases, adjustments can be made to the conversion.

Note that equation (6) is valid for any doping level or minority-carrier-injection level. A plot of irradiance vs. implicit voltage will show the different ideality factors from all possible injection-dependent effects without additional assumptions. This is in contrast to lifetime data, because the definition of "lifetime" becomes ambiguous due to the changing device physics at each injection level.

When using a slowly varying flash instead of a true steady-state illumination, care must be taken that errors are not introduced into the analysis by the deviations from steady-state conditions. The illumination intensity vs. time is shown for a typical pulse in Fig. 1. A numerical solution for the time-dependent photoconductance that would result from this light profile was compared to the steady-state equations 2-5 to evaluate the possible error. For minority-carrier lifetimes less than 60 μs, the error is less than one percent. This indicates an applicability of the quasi-steady-state technique of nearly 4 orders of magnitude from about 10 ns to 60 μs. The error increases to 10% for 230-μs minority-carrier effective lifetimes. To maintain this accuracy, data must be discarded prior to a

time equal to three minority-carrier lifetimes after the peak light intensity.

Experimental applications of the technique:

Photoconductance instruments operating at 10 MHz were used for this work. A coil coupled to the conductivity of the wafer and a signal proportional to this conductivity was observed on a digital oscilloscope and transferred to a computer for analysis. The voltage signal was verified to be linear in wafer conductivity over the entire range of interest. The light source was a flash lamp with a 2.3 ms time decay constant capable of irradiances exceeding 100 W/cm^2, or 1000 suns.

The techniques described above were applied to process monitoring through several stages of a BSF cell fabrication process. Results for a P-type, 1-Ω-cm, FZ wafer from this run are given in Fig. 3. After phosphorus diffusion plus oxidation (with the diffused region on both sides of the wafer) the effective lifetime is quite high, 340 μs, and can be interpreted as a lower bound on the lifetime of the bulk silicon material. After aluminum alloying at the rear and contact window opening at the front) the effective lifetime decreases significantly, mainly due to the additional recombination in the aluminum doped rear p+ region. The experiment points out that the limiting factor in the cell voltage for this particular process schedule and material is the aluminum alloying step. The sample is at this stage practically equivalent to the finished solar cell.

In Fig. 3 we display this data in the form of illumination-implied V_{oc} curves. After the initial P-diffusion step, the implied I-V_{oc} curve has an unity ideality factor from 0.3 to 5 suns illumination. The implied V_{oc} at one sun for the wafer at this stage in the process is 686 mV. After the Al diffusion on the rear of the cell, the V_{oc} curve has lost 64 mV at one sun, down to 622 mV. The ideality factor is still one. After the grids were applied, the actual V_{oc} was found to be 620 mV, in excellent agreement with the value from the quasi-steady-state photoconductance data. This agreement verifies the validity of displaying photoconductance data in the form of implied voltage.

An example of application to multicrystalline silicon is shown in Fig. 4. The 1 Ω-cm, 215 μm-thick wafer from Eurosolare was passivated with a phosphorus diffusion and oxidation. The minority carrier effective lifetime measured with the quasi-steady-state method is remarkably high: 65 μs at one sun illumination, increasing to about 80 μs at 10 suns. The implied IV curve in Fig 4 indicates that this wafer is capable of producing a solar cell with an open-circuit voltage greater than 640 mV if processed with a high-efficiency cell design. The shape of the "IV curve", taken with this contactless technique, contains far more information than would be evident in a typical lifetime measurement technique. Although the Eurosil wafer in Fig. 4 showed no evidence of them, carrier trapping effects can complicate lifetime measurements in some multicrystalline material at low light intensities [2], Fig. 5 corresponds to a finished multicrystalline cell with the metalization stripped. Here we show the inverse lifetime vs. minority-carrier density. At high carrier densities, this sample has a constant lifetime of 14 μs. However, at low carrier densities, the data indicate an anomolously high lifetime. This may be due to trapping in the grain boundaries and defects, a phenomenon that has also been observed using transient photoconductance decay [2].

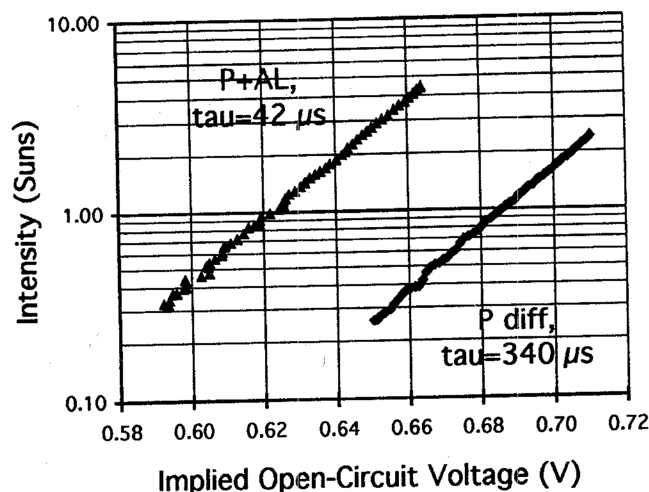

Fig. 3. The implied V_{oc} vs. Illumination curves at two points during a BSF cell fabrication sequence. The actual V_{oc} after cell completion was 620 mV.

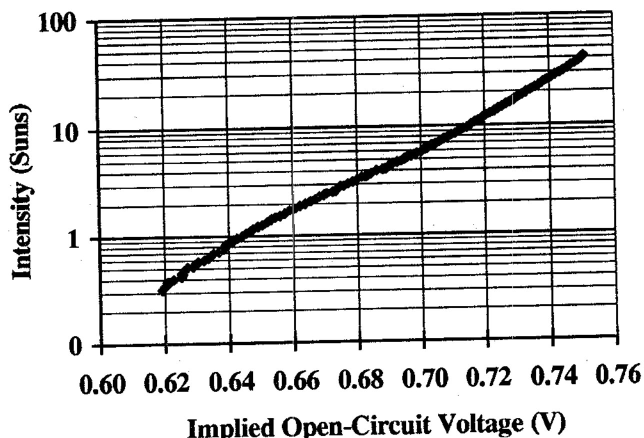

Fig. 4. The implied I-V curve for a Eurosil 1 Ω-cm wafer passivated by phosphorus diffusion and oxidation.

Clearly, these trapping effects are material dependent. Preliminary results indicate it may be useful to simply ignore data taken at low minority-carrier densities, and correlate the lifetime measured at high carrier densities to the cell properties. This approach is demonstrated in Fig 6, that shows the final dark I-V and Isc-Voc

characteristics for the same multicrystalline device used in Fig 5. An extrapolation of the implied "IV curve" (with the metalization stripped) from the high-voltage regions predicts the cell parameters quite well. An alternative method for dealing with samples that suffer from slow trapping effects might be to use a longer light pulse, or use a true steady-state light source.

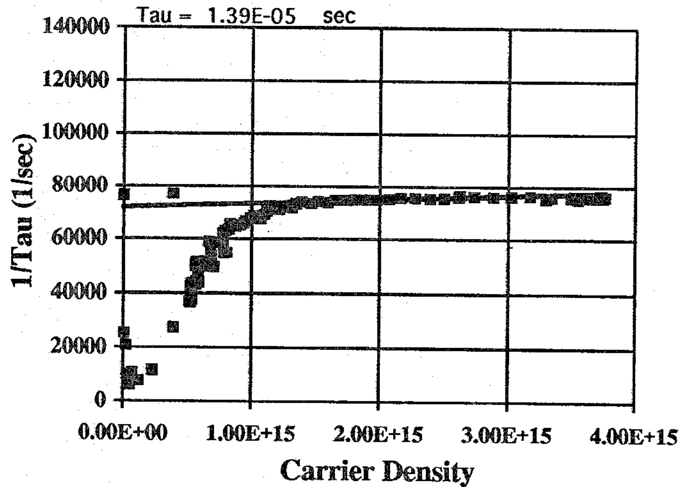

Fig. 5. The inverse of lifetime vs. carrier density for a finished multicrystalline solar cell.

Conclusions:

The quasi-steady state photoconductance method has numerous applications for process monitoring during solar cell fabrication. The substrate and passivation quality can be evaluated for individual fabrication steps beginning with the initial material quality. Besides providing an effective lifetime parameter, the measurement gives an Irradiance-Voltage curve that can be correlated to the final device characteristics. All the injection-level dependence of the recombination mechanisms is displayed in this curve. Except for effects related to the flow of an electric current, like series and contact resistance, and the short-circuit current, many relevant parameters of a solar cell, including the open-circuit voltage, saturation current density and ideality factor can be determined without depositing the metallic contacts or using patterning techniques. The measurement is practically temperature independent.

The method is simple and the data have a clear physical interpretation. It is compatible with the transient photoconductance decay approach and offers a means of extending measurement capabilities to very low lifetimes with the same apparatus. It has several additional advantages:

- The light source can be inexpensive, since it has no special requirements for short duration or sharp cut-off.

- Even when measuring lifetimes less than 1 μs, the data acquired is from a 2.3 ms decaying waveform, eliminating the fast electronics required for a transient decay measurement.

-The result depends upon the absolute value of a small signal, rather than it's derivative.

-In the range of applicability, it is effectively a steady-state measurement, similar to the cell in actual operation. The recombination components are weighted as in the actual cell under open-circuit voltage conditions including the transport and non-uniform photogeneration effects on the carrier-density profiles.

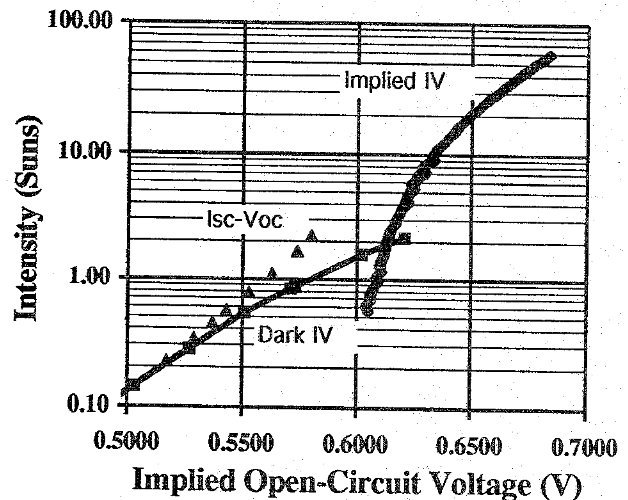

Fig. 6. Comparison of the Dark I-V and Isc-Voc curve for a finished multicrystalline cell to the implied illumination-Voc curve as calculated from photoconductance data after removing the front and rear metalization.

Acknowledgments: The authors would like to thank K. Weber, G. Matlakowski, M. Stocks and A. Carr, from the Australian National University, and Francesca Ferrazza of Eurosolare for supplying some of the samples used in this work. ANU's participation has been partially supported by the Australian Research Council.

[1] D.K. Schroder, *Semiconductor Material and Device Characterization*, Wiley, New York, 1990.

[2] R.K. Ahrenkiel, B. M. Keyes, and D. L. Levi, Recombination Processes in Polycrystalline Photovoltaic Materials, *Proc. 13th European Photovoltaic Solar Energy Conf*, Nice 23-27 October, 1996, pp 914-917.

[3] D. E. Kane and R. M. Swanson, "Measurement of the Emitter Saturation Current by a Contactless Photoconductivity Decay Method", *Proc. 18th IEEE Photovoltaics Specialist Conference*, pg 578-583, Las Vegas, NV., 1985.